GEOLOGY | THE GEOLOGICAL SOCIETY OF AMERICA®

https://doi.org/10.1130/G49310.1

Manuscript received 23 February 2021
Revised manuscript received 24 May 2021
Manuscript accepted 18 June 2021

Published online 12 August 2021

Diverse gas composition controls the Moby-Dick gas hydrate system in the Gulf of Mexico

Alexey Portnov[1], A.E. Cook[2] and S. Vadakkepuliyambatta[3]
[1]Institute for Geophysics, University of Texas, Austin, Texas 78758, USA
[2]School of Earth Sciences, The Ohio State University, Columbus, Ohio 43210, USA
[3]Center for Arctic Gas Hydrate, Environment and Climate (CAGE), Department of Geosciences, UiT–The Arctic University of Norway, Tromsø N-9037, Norway

ABSTRACT

In marine basins, gas hydrate systems are usually identified by a bottom simulating reflection (BSR) that parallels the seafloor and coincides with the base of the gas hydrate stability zone (GHSZ). We present a newly discovered gas hydrate system, Moby-Dick, located in the Ship Basin in the northern Gulf of Mexico. In the seismic data, we observe a channel-levee complex with a consistent phase reversal and a BSR extending over an area of ~14.2 km², strongly suggesting the presence of gas hydrate. In contrast to classical observations, the Moby-Dick BSR abnormally shoals 150 m toward the seafloor from west to east, which contradicts the northward-shallowing seafloor. We argue that the likely cause of the shoaling BSR is a gradually changing gas mix across the basin, with gas containing heavier hydrocarbons in the west transitioning to methane gas in the east. Our study indicates that such abnormal BSRs can be controlled by gradual changes in the gas mix influencing the shape of the GHSZ over kilometers on a basin scale.

INTRODUCTION

Gas hydrate, a clathrate of natural gas and H_2O, is stable on continental slopes worldwide in a near-seafloor interval called the gas hydrate stability zone (GHSZ). The thickness and hydrate occurrence in the GHSZ can be used to quantify the global hydrate reservoir and understand the influence of that reservoir in the global carbon cycle (Wallmann et al., 2012; Ruppel and Kessler, 2016). The base of the GHSZ is a critical thermodynamic boundary between overlying gas hydrate and underlying free gas, which is a function of four components: pressure, temperature, gas composition, and salinity (Kvenvolden, 1993; Kvenvolden and Lorenson, 2001). In marine seismic data, the base of the GHSZ is often inferred from a bottom simulating reflection (BSR), a seafloor-parallel seismic reflection caused by free gas under the base of the GHSZ (Shipley et al., 1979; Haacke et al., 2007).

In a classical gas hydrate system, the base of the GHSZ parallels the seafloor. Assuming salinity and gas composition are constant, it is possible to estimate the geothermal gradient from the BSR depth, and this has been done in several locations with varying success (e.g., Grevemeyer and Villinger, 2001; Phrampus et al., 2017). Yet, in salt tectonic provinces like the Gulf of Mexico, salt bodies, fluid flow, and faulting can distort the heat flow and salinity even on a reservoir scale (Ruppel et al., 2005; Forrest et al., 2007; Wilson and Ruppel, 2007; Portnov et al., 2020). A BSR deviating from the seafloor-parallel depth path suggests that there is local heterogeneity in the near-seafloor system, which could be caused by variations in temperature, salinity, and/or gas mix.

Pure methane gas has the shallowest base of GHSZ, but it deepens even if a small amount of higher-order hydrocarbons, such as ethane (C_2) or propane (C_3), is present (Sloan and Koh, 2007). Microbial methane is often found in near-seafloor sediments, generated in place by microbes consuming organic matter (Floodgate and Judd, 1992) or recycled at the base of the GHSZ (Nole et al., 2018). In contrast, thermogenic gas with higher-order hydrocarbons transported buoyantly through faults and chimneys is often detected in gas chimneys and hydrate mounds on the seafloor (Brooks et al., 1984; Macdonald et al., 1994; Sassen et al., 2001). In seismic data, thermogenic gas is generally only inferred at a location due to the presence of gas chimneys or double BSRs, i.e., two or more stacked reflections indicating shallower methane and deeper thermogenic boundaries of gas hydrate stability (Posewang and Mienert, 1999; Andreassen et al., 2000; Foucher et al., 2002; Pohlman et al., 2005; Paganoni et al., 2016; Plaza-Faverola et al., 2017; Bertoni et al., 2019; Minshull et al., 2020).

We argue that in contrast to a double BSR, the BSR depth can change gradually across kilometers in a basin reflecting a smooth change in gas composition. We used three-dimensional (3-D) seismic and well-log data to characterize a new gas hydrate system, Moby-Dick, in a channel-levee complex in the northern Gulf of Mexico. We argue that at Moby-Dick, an increase of thermogenic gas input from gas chimneys in the western side of the basin is a likely explanation for the smooth westward deepening of the GHSZ base.

DATA AND METHODS

We used a time-migrated 3-D seismic survey, B-20–92-LA, and 2-D line W-LS-389A_E publicly available at the National Archive of Marine Seismic Surveys (https://walrus.wr.usgs.gov/namss/; see the Supplemental Material[1]). Resistivity, gamma ray, gas chromatographic logs, permit documents, and drilling operations

[1]Supplemental Material. Information about the sources and processing characteristics of the public seismic, well log, and gas chromatography data; and time-depth conversion parameters, velocity model, and calculations of geothermal gradients. Please visit https://doi.org/10.1130/GEOL.S.15062322 to access the supplemental material, and contact editing@geosociety.org with any questions.

CITATION: Portnov, A., Cook, A.E., and Vadakkepuliyambatta, S., 2021, Diverse gas composition controls the Moby-Dick gas hydrate system in the Gulf of Mexico: Geology, v. 49, p. 1446–1451, https://doi.org/10.1130/G49310.1

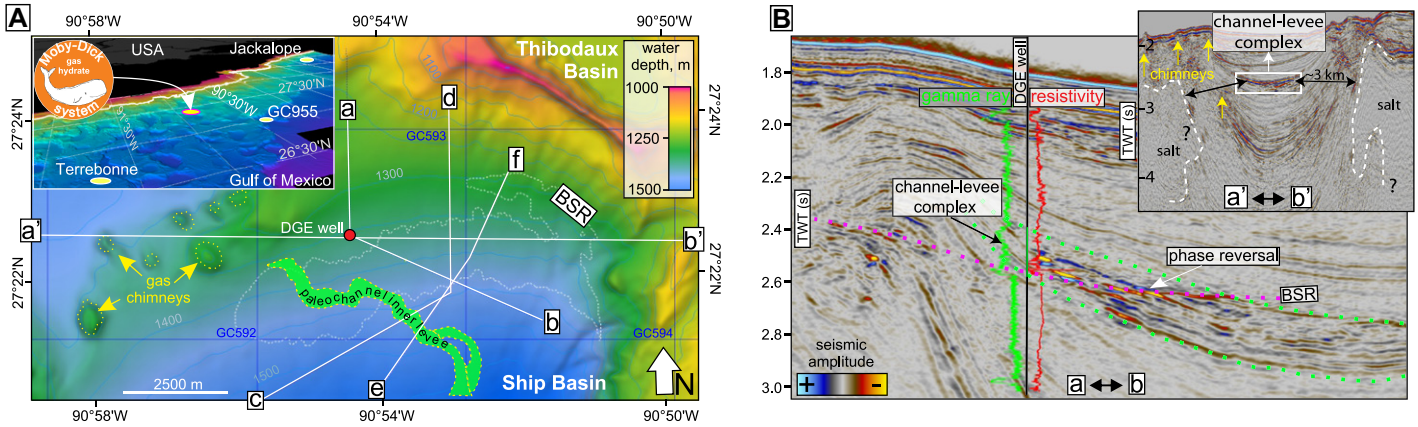

Figure 1. (A) Seafloor bathymetry map showing the areal extent of the Moby-Dick gas hydrate system, including a paleochannel, bottom simulating reflection (BSR), and deeply rooted gas chimneys that may potentially supply thermogenic gas to the Moby-Dick system. Inset: Location of the Moby-Dick system relative to other gas hydrate systems in the Gulf of Mexico. (B) Channel-levee complex in seismic and well-log data (green dotted interval) is crosscut by bottom simulating reflection (BSR; purple dotted line). Location of cross section a-b is shown in Figures 1A and 3A. Inset: Location of channel-levee complex in the central part of the minibasin where salt-related temperature and salinity variations are minimal. Location of the cross section a′-b′ is shown in A.

reports from a Deep Gulf Energy (DGE; Houston, Texas, USA) well (API 608114053100) were acquired from the U.S. Bureau of Safety and Environmental Enforcement (https://www.bsee.gov). The velocity model for the seismic-well tie and all time-depth conversions were based on the density and velocity functions derived for marine mud sediments by Cook and Sawyer (2015) (see the Supplemental Material). Spatial modeling of geothermal gradients over the mapped BSR surface was based on the depth of the BSR below the seafloor (see the Supplemental Material).

RESULTS AND DISCUSSION

Geologic Setting

The Moby-Dick gas hydrate system is located in water depths of 1250–1480 m in the Ship Basin in the northern Gulf of Mexico (Fig. 1). In seismic data, salt bodies are evident at the basin margins (>3000 m away from the Moby-Dick system), yet in the central portion of the basin, the salt surface is not resolved, indicating that it is extremely deep (>6 s two-way traveltime [TWT]; Fig. 1B). West of Moby-Dick, a group of seven deep-rooted gas chimneys form mounds at the seafloor, up to 1000 m wide and 100 m tall, possibly representing gas hydrate pingos or mud volcanos (Fig. 1A).

BSR in a Channel-Levee Complex

The Moby-Dick hydrate system is characterized by a prominent and consistent trough-leading BSR (Figs. 1B and 2A) extending over 14.2 km^2 (Fig. 1A). The BSR is discontinuous at the northern margin of the Ship Basin, yet in the central part of our study area, the BSR becomes more coherent and crosscuts the sedimentary bedding. The BSR occurs within an ~200–250-m-thick seismic unit with high-amplitude reflections associated with a coarse-grained channel depositional system (Figs. 2A–2C). The channel complex is underlain by a prominent basal horizon deposited prior to the onset of the channel (Figs. 2A–2C). We flattened the seismic volume along the basal horizon to simulate the paleo-seafloor and visualize the original configuration of the channel complex (Figs. 2B and 2C). This showed channel deposits extending ~3500 m on both sides of an ~1000-m-wide channel with outer levees up to 250 m thick (Figs. 2B and 2C). Frequency spectral decomposition showed the high-sinuosity axis of the major channel extending in a general northwest-southeast direction (inset of Fig. 2C), as well as several meandering channel paths deviating from its primary trajectory (inset of Fig. 2C; Fig. 3). The DGE well was drilled into the eastern outer levee (Figs. 1B and 2C) and shows an ~150-m-thick coarse-grained interval with low gamma ray (35–55 API) corresponding to a unit in the seismic data interpreted as channel deposits (Figs. 1B and 2C). In summary, the Moby-Dick system is associated with a coarse-grained channel-levee complex up to 250 m thick, favorable for gas and hydrate accumulations.

The seismic pattern of the channel-levee complex comprises several continuous horizons likely corresponding to sand intervals. The Whalebone Horizon is the most prominent and is present over the entire channel-levee complex (Fig. 3A). In the Whalebone Horizon, we observed a change in the seismic response from high-amplitude peak-leading reflection above the BSR to trough-leading reflection below (Figs. 1B and 3A). This phase reversal is sharp and consistent and extends over ~9 km from east to west across the basin (Fig. 3A). Such a seismic configuration indicates a gas hydrate–bearing sand associated with the peak-leading reflection above the BSR changing to a gas-bearing sand and a trough-leading reflection below the BSR (Boswell et al., 2012; Hillman et al., 2017). Below the Whalebone Horizon, we observed the peak-leading Ship Horizon with a phase reversal (inset of Fig. 3A; Fig. 3B) occupying an approximate area of 2.5 km^2. A map of peak-leading amplitudes above the BSR surface shows the approximate gas hydrate distribution above the base of the GHSZ in both horizons (Fig. 3B). The strongest peak-leading amplitudes are likely associated with the highest hydrate saturation. A similar map for trough-leading amplitudes below the BSR surface shows distribution of free gas below the base of the GHSZ (Fig. 3C).

At Moby-Dick, there are no wells drilled into the potential hydrate-bearing horizons. The DGE well was drilled ~150 m away from the closest high-amplitude peak-leading reflections (Fig. 3A). Due to a flow observed at the wellhead when the drill bit approached the base of the GHSZ (~685 m below seafloor, 2031 m measured depth [MD]), casing was installed over the GHSZ, corrupting the well-log data (Figs. S1A and S1B in the Supplemental Material). The flow observed at the wellhead could have been caused by excess formation pore pressure due to free gas at the base of the GHSZ.

Geothermal Gradient and Gas Composition

If we assume Moby-Dick is a classic methane hydrate system with 100% methane gas and standard seawater salinity of 35 g/L, we estimate a 24 °C/km geothermal gradient from the BSR depth in the eastern part of Moby-Dick. The modeled base of the GHSZ suggests the BSR should gradually deepen by ~25 m from north to south due to the southward seafloor deepening (Fig. 1A). Instead, the Moby-Dick BSR deepens by ~150 m relative to the seafloor from east to west (Fig. 4A).

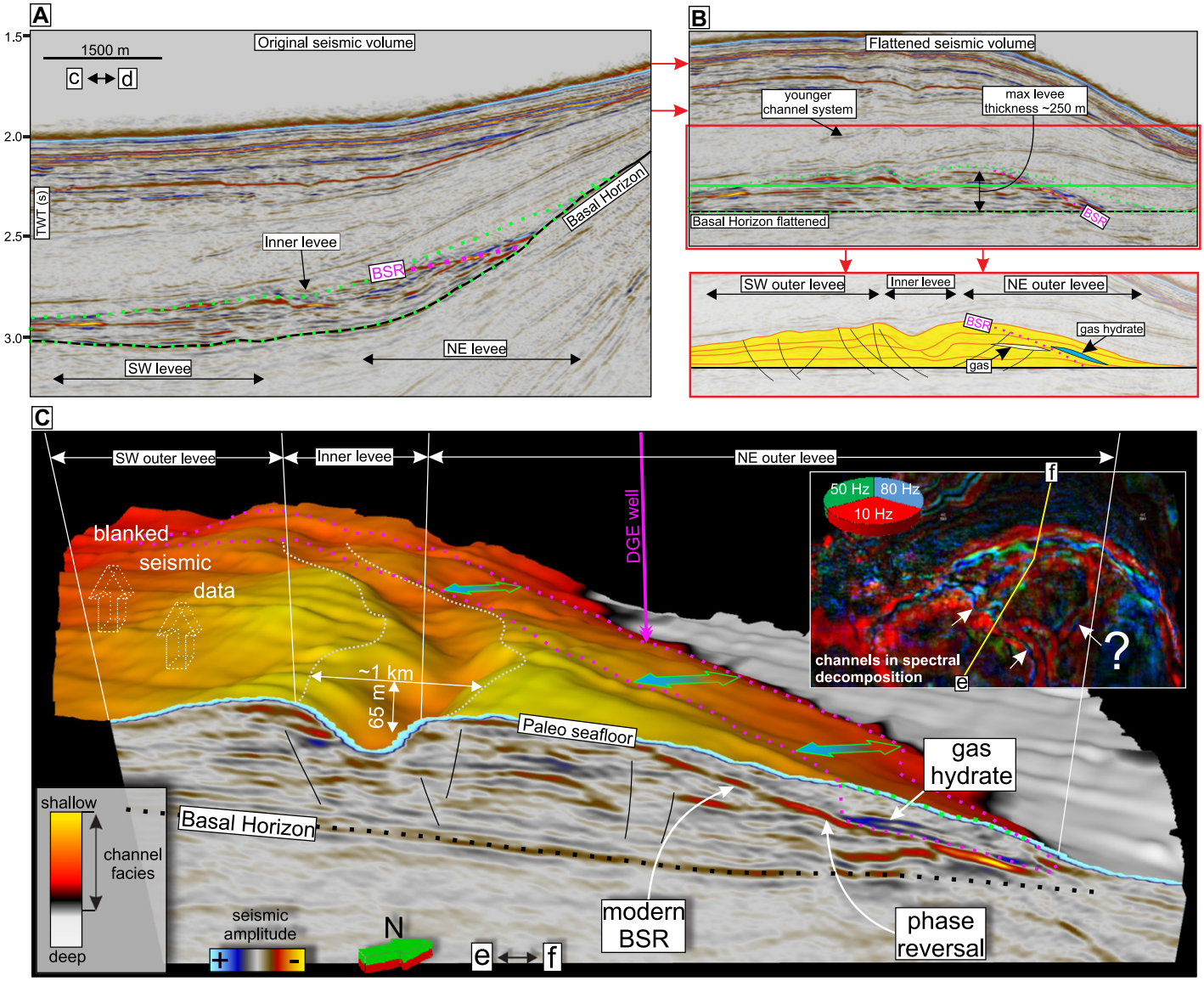

Figure 2. (A) Seismic cross section c-d (see Fig. 1A for location) showing bottom simulating reflection (BSR) and phase reversal within the channel-levee complex (green dotted interval). Black solid line shows the basal horizon used for seismic volume flattening. (B) Cross section c-d in flattened seismic volume showing major elements of depositional and gas hydrate systems. Green solid line shows the depth slice used for frequency spectral decomposition. (C) Three-dimensional visualization of the channel-levee complex across an arbitrary section e-f (see Fig. 1A) in a flattened seismic cube, blanked above the complex surface. Inset: Channel configuration and location of section e-f in frequency spectral decomposition map.

There are several factors that could cause the abnormal BSR depth across the Ship Basin: distortion of seismic reflectors in time-migrated seismic data, elevated pore pressure in the west, significant salinity variations, a variable geothermal gradient, and variable gas composition. To test the possible distortion of seismic reflectors, we constructed a velocity model to convert the time-migrated east-west seismic section to depth (Figs. S2A and S2B). This model shows that any velocity effects within the GHSZ that could explain the observed BSR configuration are negligible (Figs. S2A and S2B). We also ruled out the possible effect of elevated pore pressure, which is normally hydrostatic in the near-seafloor sediments (Osborne and Swarbrick, 1997). Moreover, a gradually elevated pressure would have to coincide exactly with the slightly dipping base of the GHSZ to provide such an effect at Moby-Dick. Finally, significant salinity variations are not common in the central parts of minibasins; in general, a seawater salinity of 35 g/L is typical for the upper ~2 km of sediment within minibasins (Wilson and Ruppel, 2007; Hanor and Mercer, 2010). Due to the distance of the Moby-Dick system from the salt bodies (~3 km) and no resistivity decrease in the DGE well log indicating high pore-water salinity (Fig. 1B), we consider that a gradual salinity increase from 35 to 67.5 g/L across the basin is unlikely.

Two factors can still explain the observed BSR configuration: a variable geothermal gradient and variable gas composition.

If we assume the gas in the system is 100% methane, a geothermal model that causes the BSR to deepen 150 m from east to west can be explained by a geothermal gradient change from ~24 to 19 °C/km from east to west (Fig. 4A). Cooling effects from higher sedimentation are highly unlikely to cause a geothermal gradient change, because seismic data show relatively uniform stratigraphic bedding from west to east (Figs. S2A and S2B). Nevertheless, such steep temperature variations can occur above heat-conductive allochthonous salt, which has

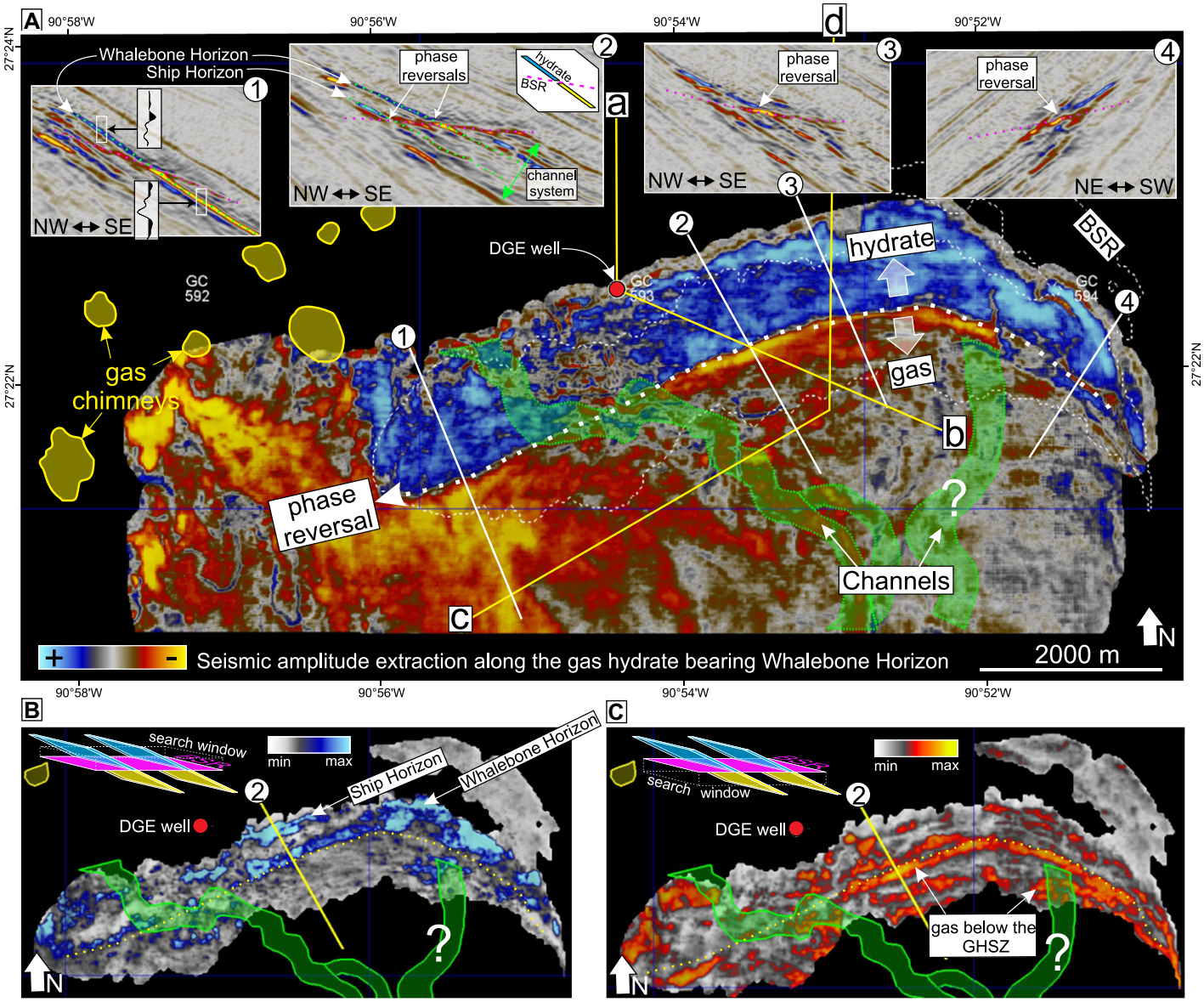

Figure 3. (A) Map of instantaneous amplitude along the hydrate-bearing Whalebone Horizon. Blue color defines the extent of peak-leading amplitudes associated with gas hydrate. Insets 1–4 show phase reversals across the Moby-Dick system. BSR—bottom simulating reflection. (B) Map of average positive amplitudes indicating gas hydrate within 30 ms (~27 m) above the base of the gas hydrate stability zone (GHSZ). (C) Map of negative amplitudes indicating gas within 30 ms (~27 m) below the base of the GHSZ.

been previously reported as a significant GHSZ distortion factor (Mello et al., 1995; Portnov et al., 2020). However, normally such geothermal anomalies are negligible or absent within central parts of minibasins, far from salt bodies (Wilson and Ruppel, 2007; Portnov et al., 2020). Furthermore, if such an effect existed at Moby-Dick, it would be bilateral due to the equidistant location of the salt bodies on either side of the gas hydrate system (Fig. 1B). Thus, a modeled ~5 °C/km lateral change in the geothermal gradient over only ~8 km distance in the central part of the basin is unlikely.

If we assume the geothermal gradient across the basin is uniform, then there would be a gradual gas composition change from 100% C_1 (most likely microbial gas) causing a shallower base of the GHSZ in the east to a gas mix resulting in a deeper base of the GHSZ in the west (Figs. 2B and 2C). This assumption is supported by multiple deep-rooted gas chimneys adjacent to Moby-Dick in the west (Fig. 1A and 3A), which likely shuttle thermogenic gas to the seafloor and may supply gas to the gas hydrate system. Moreover, strongly negative seismic amplitudes are much more abundant within the western part of the Whalebone Sand (Fig. 3A), confirming a higher gas concentration in the proximity of the gas chimneys.

In this case, however, many non-unique combinations of gas mix could match the BSR depth depending on the concentration of heavier hydrocarbons (C_2–C_5) in the total gas composition. Analyses of the gas chromatographic logs from the sub-GHSZ interval in the DGE well revealed corrupted C_1–C_5 records due to incorrect machine calibration and failure (Fig. S3). Therefore, we modeled a plausible sequence of changing synthetic gas mixes along the west-east shoaling BSR (Figs. 4B and 4C), which vary the concentration of C_2 and C_3 at a 2:1 ratio (a realistic ratio for deep-water Gulf of Mexico; Thiagarajan et al., 2020). In such scenario, a gradual depletion of heavier hydrocarbons will smoothly shoal the base of the GHSZ eastward and slightly updip. This produces a single shoaling BSR without generating a double BSR, such as that observed in other gas hydrate systems of possible thermogenic nature (Fig. 4C; Posewang and Mienert, 1999; Andreassen et al., 2000; Foucher et al., 2002).

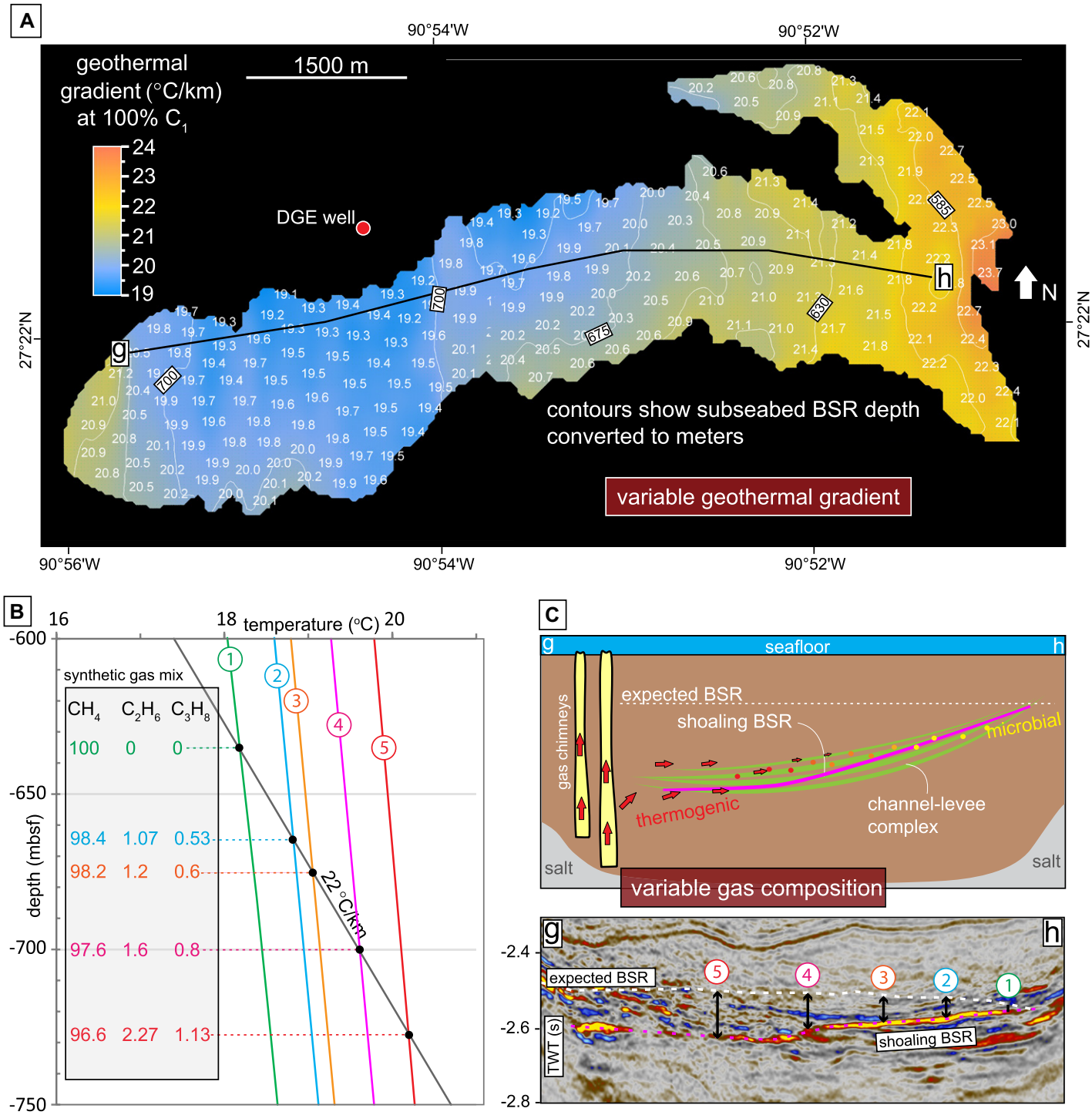

Figure 4. (A) Geothermal gradient model based on observed bottom simulating reflection (BSR) depth (labeled white contours) and microbial gas composition (100% C_1) range between 23.7 and 19.2 °C/km. Location of line g-h is shown. (B) Gas hydrate phase boundaries from synthetic gas mix including C_2 and C_3 (2:1 ratio) gradually depleting eastward (mbsf—m below seafloor). Diagram shows possible shoaling of the gas hydrate stability zone (GHSZ) lower boundary given uniform geothermal gradient. (C) Possible injection of thermogenic gas into the channel-levee complex causes deeper BSR in the west and a gradual transition from a thermogenic to microbial system eastward (line g-h).

CONCLUSIONS

The Moby-Dick gas hydrate system includes two hydrate-bearing horizons in a channel-levee complex. We interpreted the presence of gas hydrate from phase reversals and peak-leading reflections above the BSR, which occupies an area of ~14.2 km². The west-to-east shoaling BSR does not mimic the seafloor, and we argue that this variation in the BSR depth is predominantly caused by a change in gas mix containing heavier hydrocarbons in the west to pure methane gas in the east. Such a configuration may indicate a west-to-east transition from a thermogenic to a microbial system. The Moby-Dick system demonstrates that the default assumption of methane hydrate may be misleading for hydrate prospecting purposes and broader estimates of the GHSZ thickness and volume.

ACKNOWLEDGMENTS

This material is based upon work supported by the U.S. Bureau of Ocean Energy Management (BOEM) award 140M0119P0041 and U.S. National Science Foundation award 1752882. S. Vadakkepuliyambatta is supported by the Research Council of Norway through its Centers of Excellence funding scheme grant 223259. We are thankful to Matt Frye, Stephen Palmes (BOEM), Lori Summa (University of Texas at Austin, USA), David Awwiller, Steve Becker, Mike Formolo (ExxonMobil), Jurgen Mienert, Ingo Pecher (University of Auckland, New Zealand), and two anonymous reviewers for help with mud-log data interpretation, fruitful discussions, and helpful suggestions.

REFERENCES CITED

Andreassen, K., Mienert, J., Bryn, P., and Singh, S.C., 2000, A double gas-hydrate related bottom simulating reflector at the Norwegian continental margin: Annals of the New York Academy of Sciences, v. 912, p. 126–135, https://doi.org/10.1111/j.1749-6632.2000.tb06766.x.

Bertoni, C., Gan, Y., Paganoni, M., Mayer, J., Cartwright, J., Martin, J., Van Rensbergen, P., Wunderlich, A., and Clare, A., 2019, Late Paleocene pipe swarm in the Great South–Canterbury Basin (New Zealand): Marine and Petroleum Geology, v. 107, p. 451–466, https://doi.org/10.1016/j.marpetgeo.2019.05.039.

Boswell, R., Collett, T.S., Frye, M., Shedd, W., McConnell, D.R., and Shelander, D., 2012, Subsurface gas hydrates in the northern Gulf of Mexico: Marine and Petroleum Geology, v. 34, p. 4–30, https://doi.org/10.1016/j.marpetgeo.2011.10.003.

Brooks, J.M., Kennicutt, M.C., Fay, R.R., McDonald, T.J., and Sassen, R., 1984, Thermogenic gas hydrates in the Gulf of Mexico: Science, v. 225, p. 409–411, https://doi.org/10.1126/science.225.4660.409.

Cook, A., and Sawyer, D., 2015, The mud-sand crossover on marine seismic data: Geophysics, v. 80, p. A109–A114, https://doi.org/10.1190/geo2015-0291.1.

Floodgate, G.D., and Judd, A.G., 1992, The origins of shallow gas: Continental Shelf Research, v. 12, p. 1145–1156, https://doi.org/10.1016/0278-4343(92)90075-U.

Forrest, J., Marcucci, E., and Scott, P., 2007, Geothermal gradients and subsurface temperatures in the northern Gulf of Mexico: Gulf Coast Association of Geological Societies Transactions, v. 55, p. 233–248, https://www.searchanddiscovery.com/pdfz/documents/2007/07013forrest/images/forrest.pdf.html.

Foucher, J.P., Nouzé, H., and Henry, P., 2002, Observation and tentative interpretation of a double BSR on the Nankai slope: Marine Geology, v. 187, p. 161–175, https://doi.org/10.1016/S0025-3227(02)00264-5.

Grevemeyer, I., and Villinger, H., 2001, Gas hydrate stability and the assessment of heat flow through continental margins: Geophysical Journal International, v. 145, p. 647–660, https://doi.org/10.1046/j.0956-540x.2001.01404.x.

Haacke, R.R., Westbrook, G.K., and Hyndman, R.D., 2007, Gas hydrate, fluid flow and free gas: Formation of the bottom-simulating reflector: Earth and Planetary Science Letters, v. 261, p. 407–420, https://doi.org/10.1016/j.epsl.2007.07.008.

Hanor, J.S., and Mercer, J.A., 2010, Spatial variations in the salinity of pore waters in northern deep water Gulf of Mexico sediments: Implications for pathways and mechanisms of solute transport: Geofluids, v. 10, p. 83–93, https://doi.org/10.1111/j.1468-8123.2009.00271.x.

Hillman, J.I.T., Cook, A.E., Daigle, H., Nole, M., Malinverno, A., Meazell, K., and Flemings, P.B., 2017, Gas hydrate reservoirs and gas migration mechanisms in the Terrebonne Basin, Gulf of Mexico: Marine and Petroleum Geology, v. 86, p. 1357–1373, https://doi.org/10.1016/j.marpetgeo.2017.07.029.

Kvenvolden, K.A., 1993, Gas hydrates—Geological perspective and global change: Reviews of Geophysics, v. 31, p. 173–187, https://doi.org/10.1029/93RG00268.

Kvenvolden, K.A., and Lorenson, T.D., 2001, The global occurrence of natural gas hydrate, *in* Paull, C.K., and Dillon, W.P., eds., Natural Gas Hydrates: Occurrence, Distribution, and Detection: American Geophysical Union Geophysical Monograph 124, p. 3–18, https://doi.org/10.1029/GM124p0003.

Macdonald, I.R., Guinasso, N.L., Sassen, R., Brooks, J.M., Lee, L., and Scott, K.T., 1994, Gas hydrate that breaches the sea-floor on the continental-slope of the Gulf of Mexico: Geology, v. 22, p. 699–702, https://doi.org/10.1130/0091-7613(1994)022<0699:GHTBTS>2.3.CO;2.

Mello, U.T., Karner, G.D., and Anderson, R.N., 1995, Role of salt in restraining the maturation of subsalt source rocks: Marine and Petroleum Geology, v. 12, p. 697–716, https://doi.org/10.1016/0264-8172(95)93596-V.

Minshull, T.A., et al., 2020, Hydrate occurrence in Europe: A review of available evidence: Marine and Petroleum Geology, v. 111, p. 735–764, https://doi.org/10.1016/j.marpetgeo.2019.08.014.

Nole, M., Daigle, H., Cook, A.E., Malinverno, A., and Flemings, P.B., 2018, Burial-driven methane recycling in marine gas hydrate systems: Earth and Planetary Science Letters, v. 499, p. 197–204, https://doi.org/10.1016/j.epsl.2018.07.036.

Osborne, M.J., and Swarbrick, R.E., 1997, Mechanisms for generating overpressure in sedimentary basins: A reevaluation: American Association of Petroleum Geologists Bulletin, v. 81, p. 1023–1041, https://doi.org/10.1306/522B49C9-1727-11D7-8645000102C1865D.

Paganoni, M., Cartwright, J.A., Foschi, M., Shipp, R.C., and Van Rensbergen, P., 2016, Structure II gas hydrates found below the bottom-simulating reflector: Geophysical Research Letters, v. 43, p. 5696–5706, https://doi.org/10.1002/2016GL069452.

Phrampus, B.J., Harris, R.N., and Tréhu, A.M., 2017, Heat flow bounds over the Cascadia margin derived from bottom simulating reflectors and implications for thermal models of subduction: Geochemistry Geophysics Geosystems, v. 18, p. 3309–3326, https://doi.org/10.1002/2017GC007077.

Plaza-Faverola, A., Vadakkepuliyambatta, S., Hong, W.-L., Mienert, J., Bünz, S., Chand, S., and Greinert, J., 2017, Bottom-simulating reflector dynamics at Arctic thermogenic gas provinces: An example from Vestnesa Ridge, offshore west Svalbard: Journal of Geophysical Research: Solid Earth, v. 122, p. 4089–4105, https://doi.org/10.1002/2016JB013761.

Pohlman, J.W., Canuel, E.A., Chapman, N.R., Spence, G.D., Whiticar, M.J., and Coffin, R.B., 2005, The origin of thermogenic gas hydrates on the northern Cascadia margin as inferred from isotopic ($^{13}C/^{12}C$ and D/H) and molecular composition of hydrate and vent gas: Organic Geochemistry, v. 36, p. 703–716, https://doi.org/10.1016/j.orggeochem.2005.01.011.

Portnov, A., Cook, A.E., Heidari, M., Sawyer, D.E., Santra, M., and Nikolinakou, M., 2020, Salt-driven evolution of a gas hydrate reservoir in Green Canyon, Gulf of Mexico: American Association of Petroleum Geologists Bulletin, v. 104, p. 1903–1919, https://doi.org/10.1306/10151818125.

Posewang, J., and Mienert, J., 1999, The enigma of double BSRs: Indicators for changes in the hydrate stability field?: Geo-Marine Letters, v. 19, p. 157–163, https://doi.org/10.1007/s003670050103.

Ruppel, C., and Kessler, J.D., 2016, The interaction of climate change and methane hydrates: Reviews of Geophysics, v. 55 p. 126–168, https://doi.org/10.1002/2016RG000534.

Ruppel, C., Dickens, G.R., Castellini, D.G., Gilhooly, W., and Lizarralde, D., 2005, Heat and salt inhibition of gas hydrate formation in the northern Gulf of Mexico: Geophysical Research Letters, v. 32, L04605, https://doi.org/10.1029/2004GL021909.

Sassen, R., Losh, S.L., Cathles, L., Roberts, H.H., Whelan, J.K., Milkov, A.V., Sweet, S.T., and DeFreitas, D.A., 2001, Massive vein-filling gas hydrate: Relation to ongoing gas migration from the deep subsurface in the Gulf of Mexico: Marine and Petroleum Geology, v. 18, p. 551–560, https://doi.org/10.1016/S0264-8172(01)00014-9.

Shipley, T.H., Houston, M.H., Buffler, R.T., Shaub, F.J., Mcmillen, K.J., Laod, J.W., and Worzel, J.L., 1979, Seismic evidence for widespread possible gas hydrate horizons on continental slopes and rises: The American Association of Petroleum Geologists Bulletin, v. 63, p. 2204–2213, https://doi.org/10.1306/2F91890A-16CE-11D7-8645000102C1865D.

Sloan, E.D., and Koh, C., 2007, Clathrate Hydrates of Natural Gases, Third Edition: Boca Raton, Florida, CRC Press, Chemical Industries, 752 p.

Thiagarajan, N., Kitchen, N., Xie, H., Ponton, C., Lawson, M., Formolo, M., and Eiler, J., 2020, Identifying thermogenic and microbial methane in deep water Gulf of Mexico reservoirs: Geochimica et Cosmochimica Acta, v. 275, p. 188–208, https://doi.org/10.1016/j.gca.2020.02.016.

Wallmann, K., Pinero, E., Burwicz, E., Haeckel, M., Hensen, C., Dale, A., and Ruepke, L., 2012, The global inventory of methane hydrate in marine sediments: A theoretical approach: Energies, v. 5, p. 2449–2498, https://doi.org/10.3390/en5072449.

Wilson, A., and Ruppel, C., 2007, Salt tectonics and shallow subseafloor fluid convection: Models of coupled fluid-heat-salt transport: Geofluids, v. 7, p. 377–386, https://doi.org/10.1111/j.1468-8123.2007.00191.x.

Printed in USA